Supporting Information

N-doped carbon-coated ultrasmall Nb_2O_5 nanocomposite with excellent long cyclability for sodium storage

Zhigao Chen, Weimin Chen*, Hongxia Wang, Zhuangwei Xiao, and Faquan Yu*

Key Laboratory for Green Chemical Process of Ministry of Education,

Hubei Key Laboratory for Novel Reactor and Green Chemistry Technology,

Hubei Engineering Research Center for Advanced Fine Chemicals,

School of Chemical Engineering and Pharmacy,

Wuhan Institute of Technology, Wuhan 430205, (P.R. China)

Corresponding author:

Email: fyu@wit.edu.cn

wmchen@wit.edu.cn.

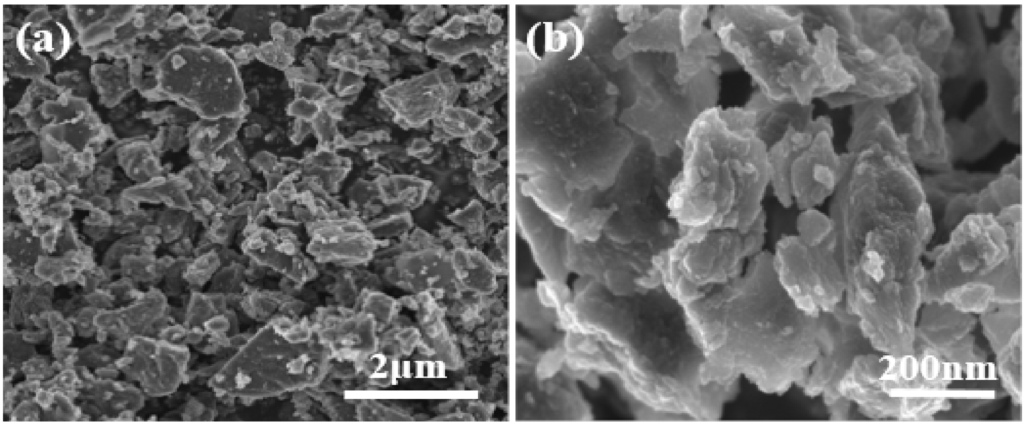

Figure S1. SEM images of 600-Nb_2O_5@NC-2.

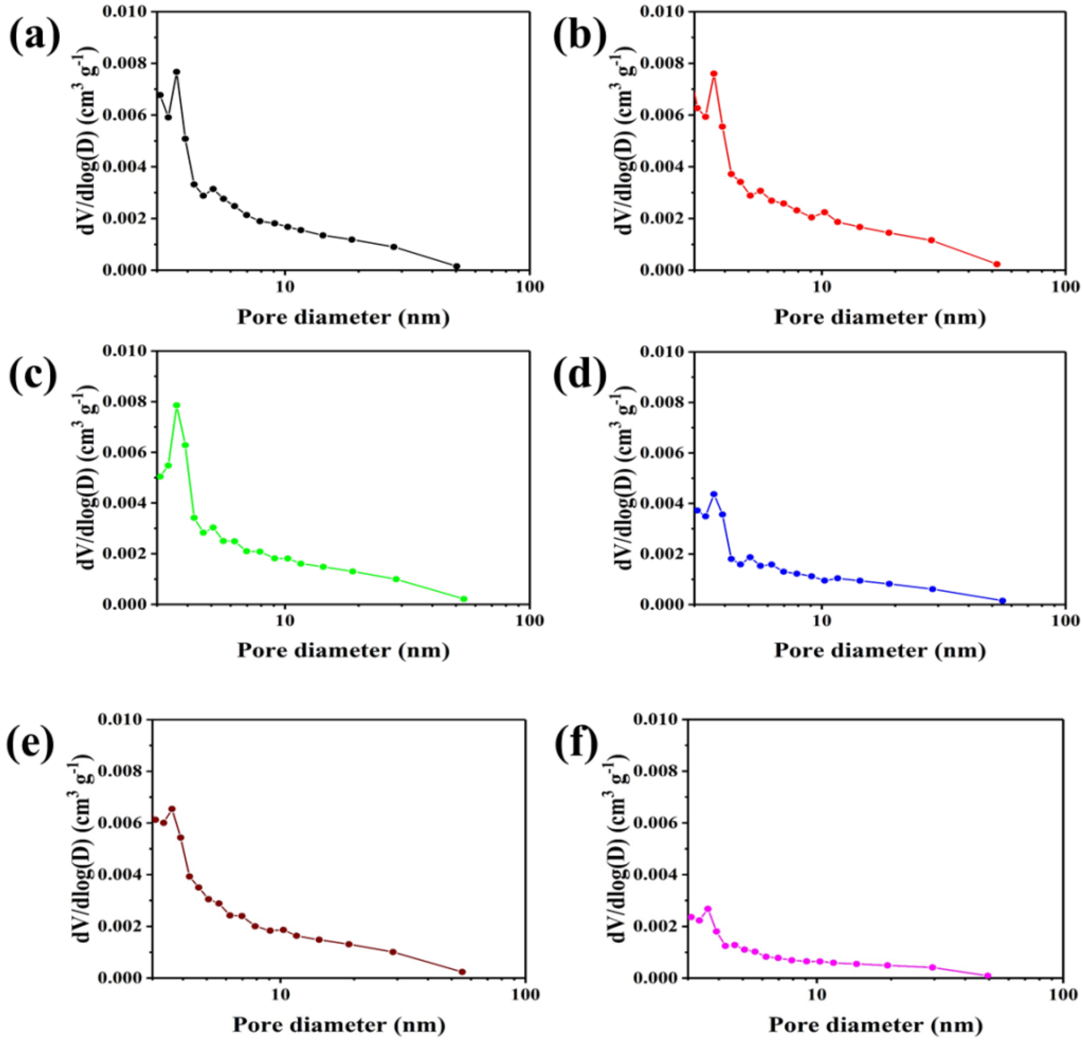

Figure S2. Pore size distribution of (a) 600-Nb_2O_5@C, (b) 600-Nb_2O_5@NC-10, (c) 600-Nb_2O_5@NC-5, (d) 600-Nb_2O_5@NC-2.5, (e) 600-Nb_2O_5@NC-2 and (f) 600-Nb_2O_5@NC-1.

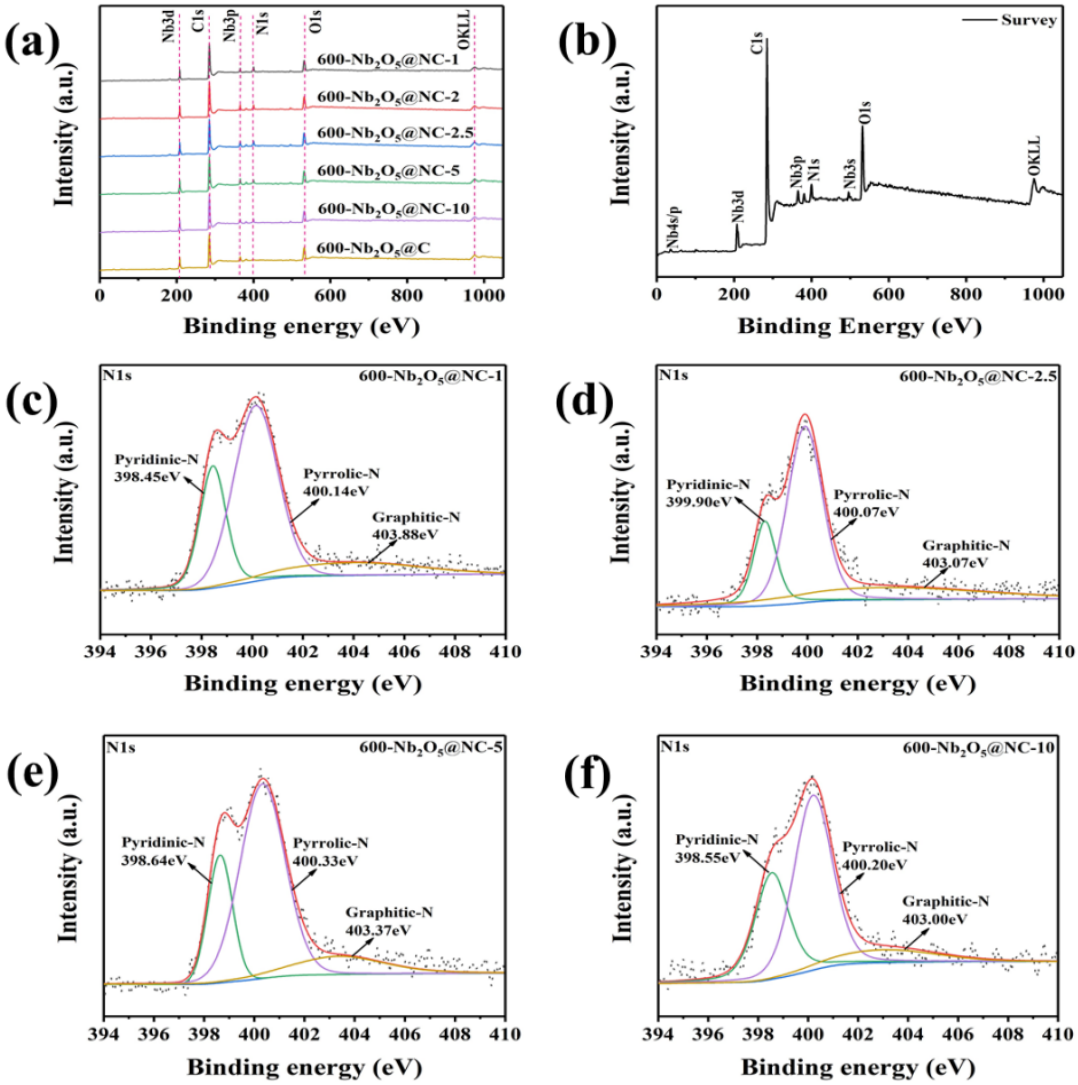

Figure S3. (a) XPS survey spectrum of the Synthetic composites of Nb_2O_5@NC and Nb_2O_5@C, (b) XPS survey spectrum of 600-Nb_2O_5@NC-2, High-resolution XPS N1s spectra of (c) 600-Nb_2O_5@NC-1, (d) 600-Nb_2O_5@NC-2.5, (e) 600-Nb_2O_5@NC-5 and (f) 600-Nb_2O_5@NC-10.

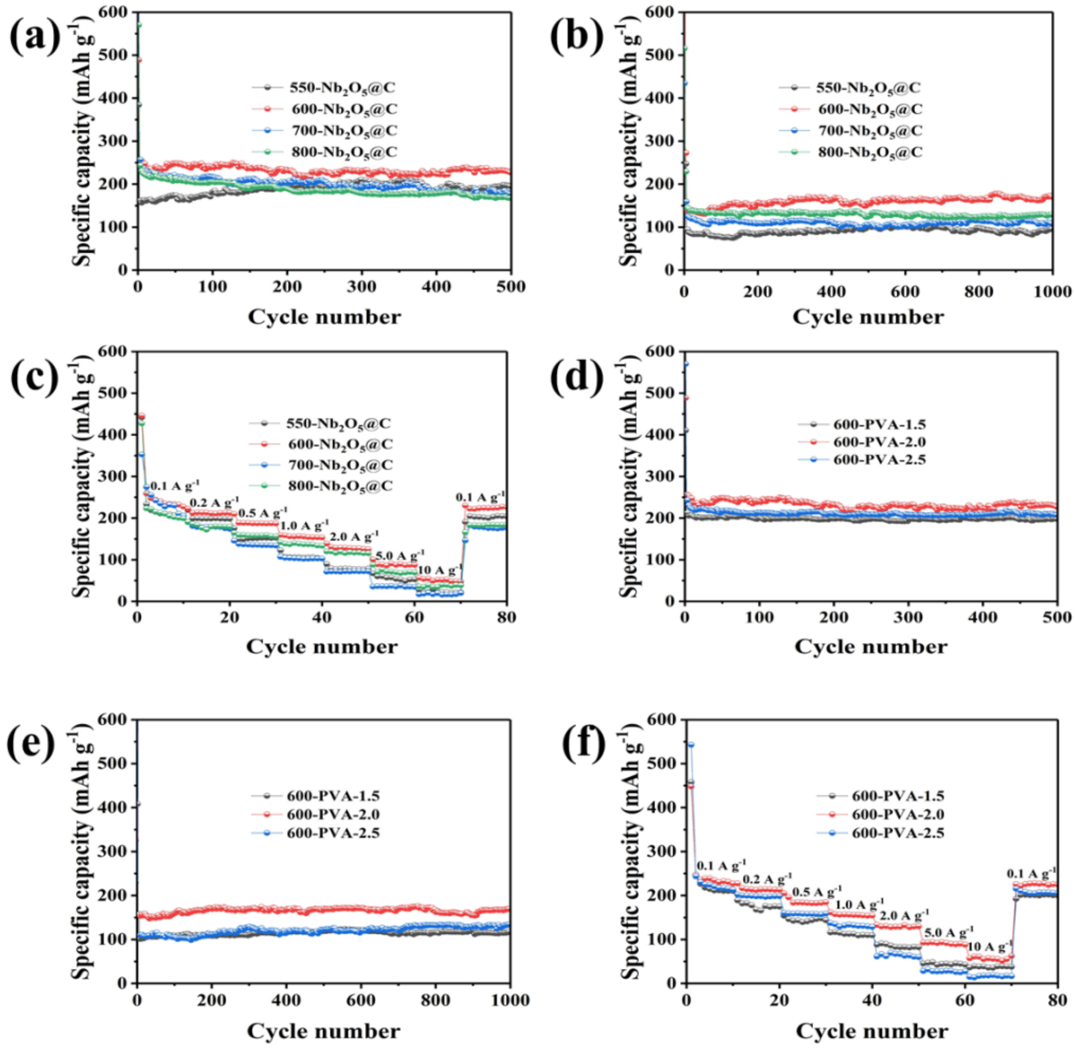

Figure S4. Exploring experiments on the effects of temperature (550-800 ℃) and PVA addition (1.5-2.5 g) on cycling performance of (a) and (d) at a current density of 0.1 A g^{-1}, (b) and (e) at a current density of 1 A g^{-1}, (c) and (f) at various current densities.

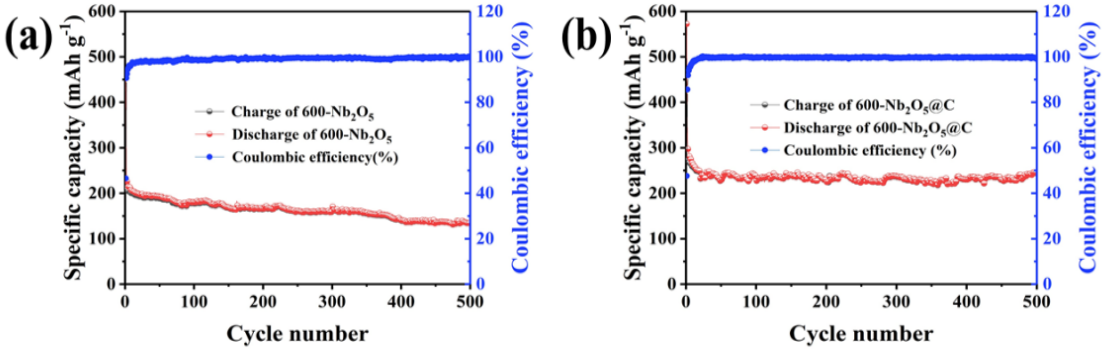

Figure S5. Cycling performances of (a) 600-Nb_2O_5 and (b) 600-Nb_2O_5@C at a current density of 0.1 A g^{-1}.

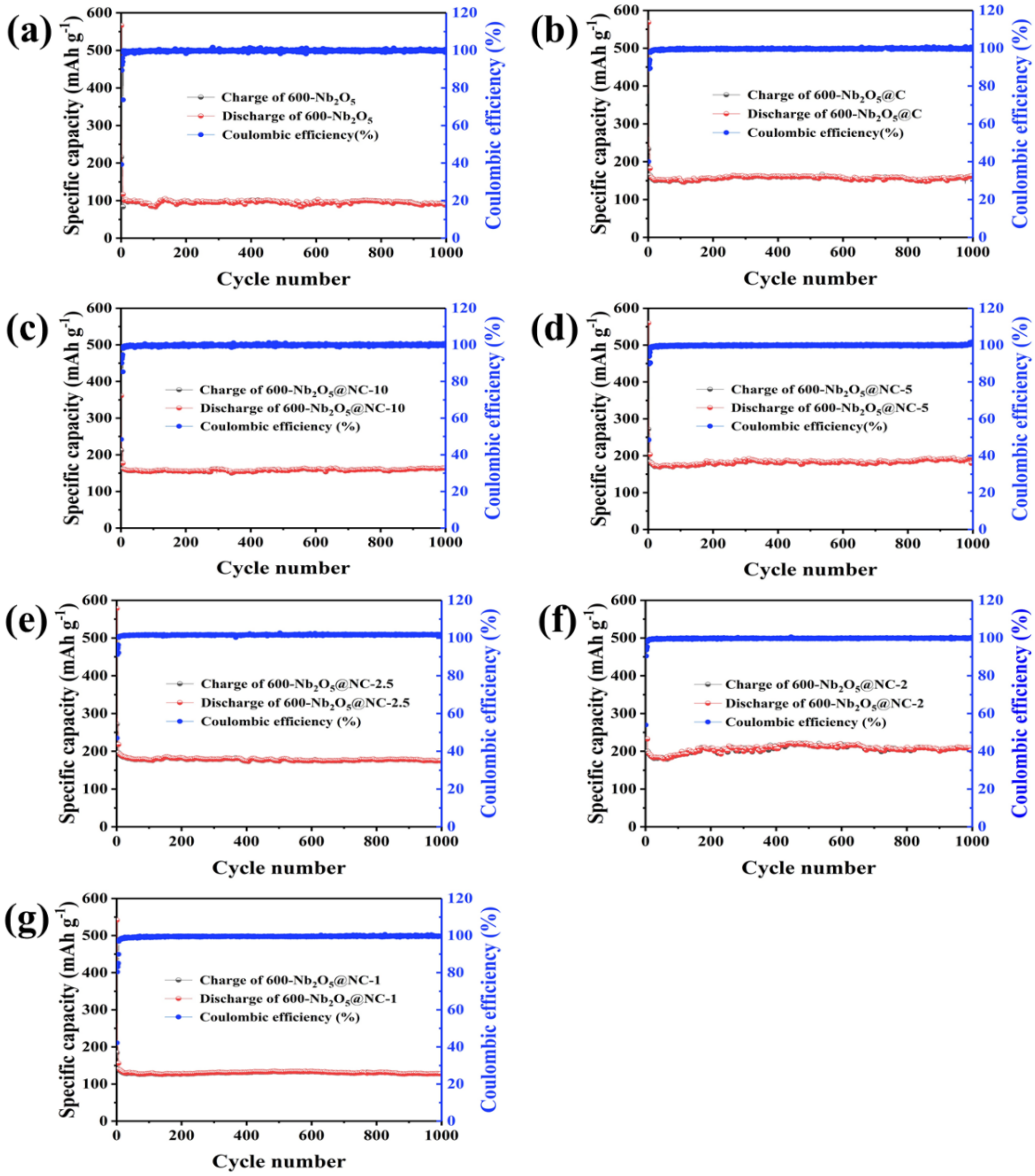

Figure S6. Cycling performances of (a) 600-Nb_2O_5, (b) 600-Nb_2O_5@C, (c) 600-Nb_2O_5@NC-10, (d) 600-Nb_2O_5@NC-5, (e) 600-Nb_2O_5@NC-2.5, (f) 600-Nb_2O_5@NC-2 and (g) 600-Nb_2O_5@NC-1 at a current density of 1.0 A g^{-1}.

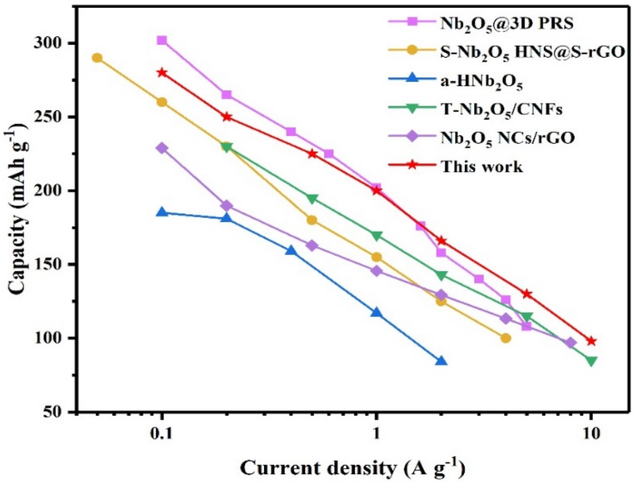

Figure S7. Comparisons between the rate performances of this work and other reported Nb_2O_5-based SIB anodes.

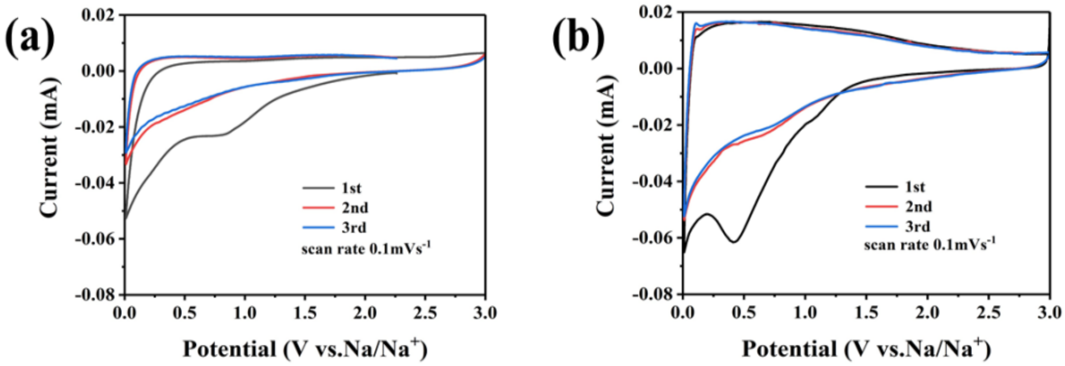

Figure S8. Cyclic voltammetry curves of (a) 600-Nb_2O_5 and (b) 600-Nb_2O_5@C at scan rates of 0.1 mV s^{-1} in the voltage range of 0.01−3 V.

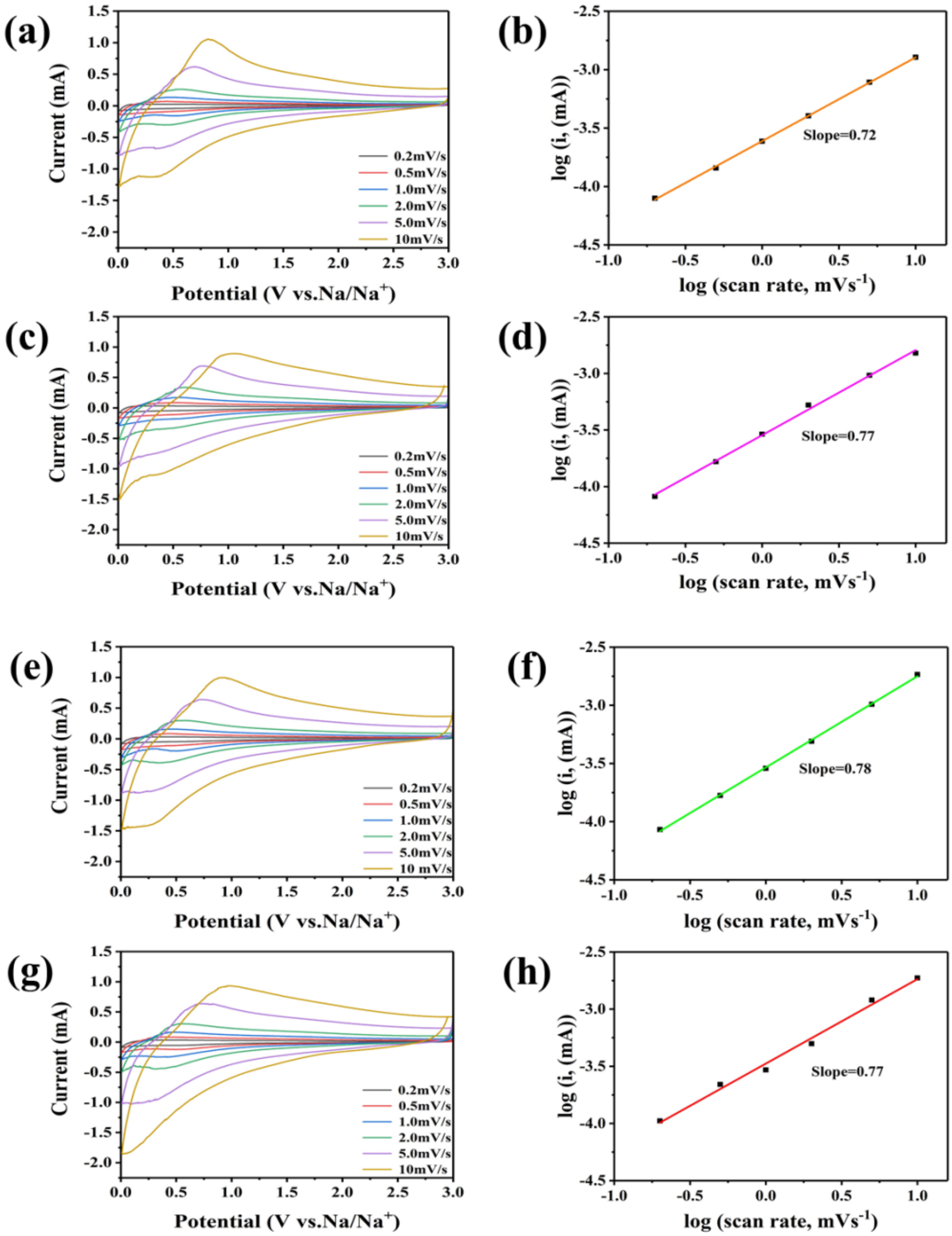
(a)
Current (mA)
Potential (V vs.Na/Na+)
0.2mV/s
0.5mV/s
1.0mV/s
2.0mV/s
5.0mV/s
10mV/s
(b)
log (i, (mA))
log (scan rate, mVs-1)
Slope=0.72
(c)
Current (mA)
Potential (V vs.Na/Na+)
0.2mV/s
0.5mV/s
1.0mV/s
2.0mV/s
5.0mV/s
10mV/s
(d)
log (i, (mA))
log (scan rate, mVs-1)
Slope=0.77
(e)
Current (mA)
Potential (V vs.Na/Na+)
0.2mV/s
0.5mV/s
1.0mV/s
2.0mV/s
5.0mV/s
10 mV/s
(f)
log (i, (mA))
log (scan rate, mVs-1)
Slope=0.78
(g)
Current (mA)
Potential (V vs.Na/Na+)
0.2mV/s
0.5mV/s
1.0mV/s
2.0mV/s
5.0mV/s
10mV/s
(h)
log (i, (mA))
log (scan rate, mVs-1)
Slope=0.77

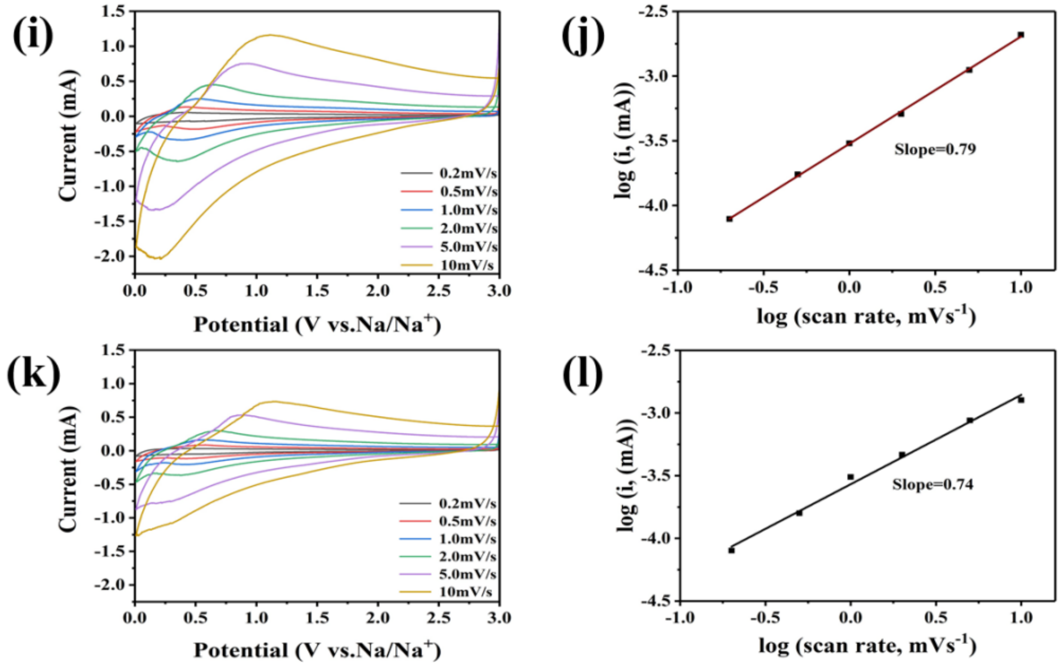

Figure S9. CV curves at various scan rates (*v*) from 0.2 to 10 mV s^{-1} for (a) 600-Nb_2O_5@C, (c) 600-Nb_2O_5@NC-10, (e) 600-Nb_2O_5@NC-5, (g) 600-Nb_2O_5@NC-2.5, (i) 600-Nb_2O_5@NC-2 and (k) 600-Nb_2O_5@NC-1. Relationship between the peak current and the scan rate (the log (*v*)-log (*i*) profiles) of (b) 600-Nb_2O_5@C, (d) 600-Nb_2O_5@NC-10, (f) 600-Nb_2O_5@NC-5, (h) 600-Nb_2O_5@NC-2.5, (j) 600-Nb_2O_5@NC-2 and (l) 600-Nb_2O_5@NC-1.

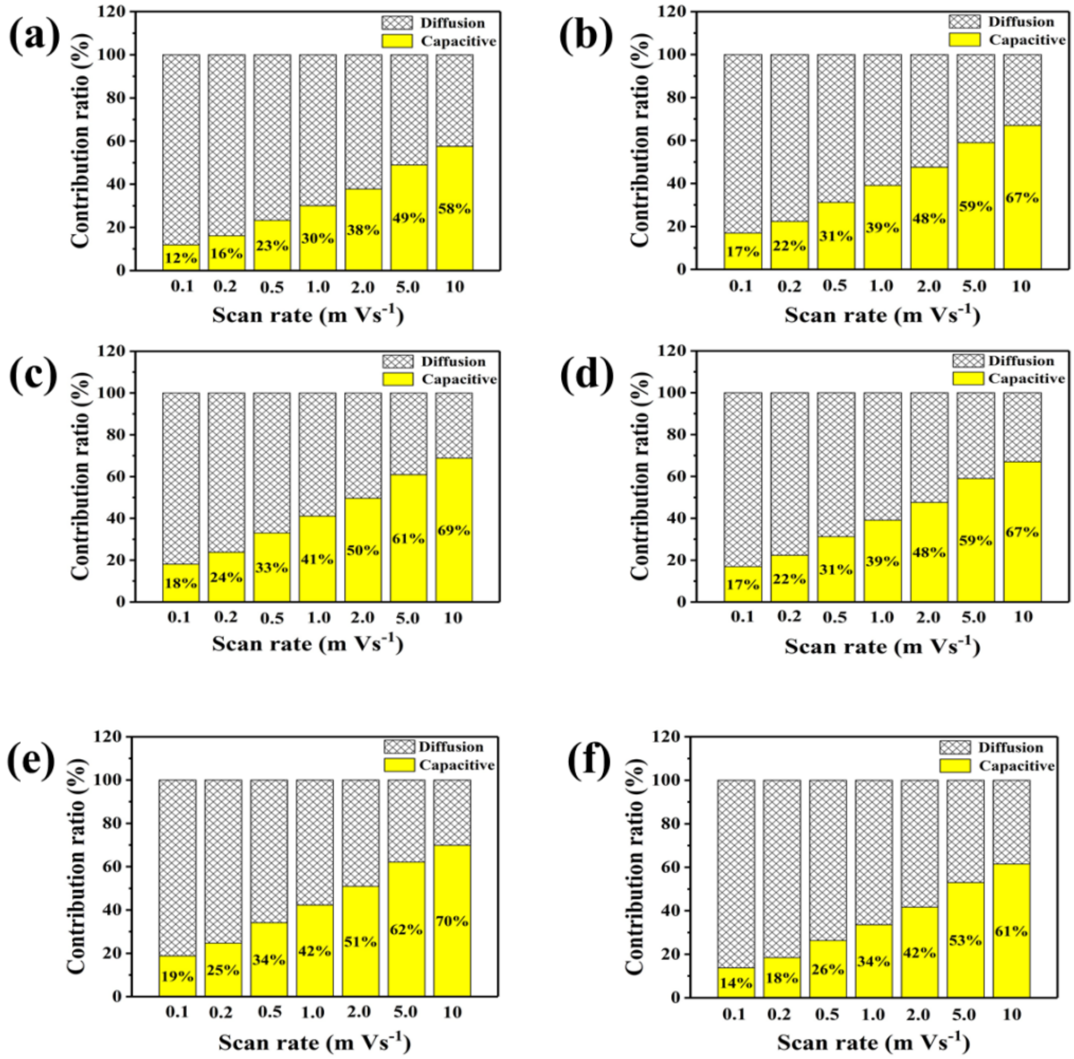

Figure S10. Contribution ratio of the capacitive and diffusion-controlled capacity versus scan rate of (a) 600-Nb_2O_5@C, (b) 600-Nb_2O_5@NC-10, (c) 600-Nb_2O_5@NC-5, (d) 600-Nb_2O_5@NC-2.5, (e) 600-Nb_2O_5@NC-2 and (f) 600-Nb_2O_5@NC-1.

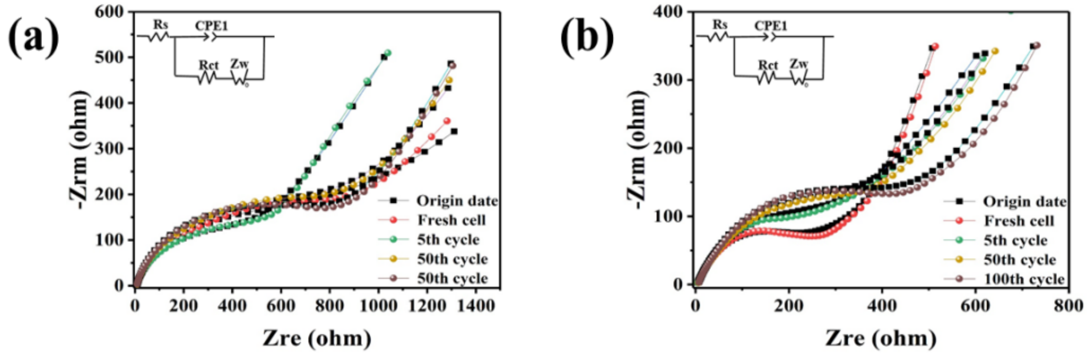

Figure S11. The Nyquist plots of (a) 600-Nb_2O_5 and (b) 600-Nb_2O_5@C electrodes before and after 5th, 50th, 100th cycles at a current density of 0.1 A g^{-1} with equivalent circuit inset.

Table S1. D-band and G-band ratios in Raman spectroscopy of composite materials

Types of materials	Raman shift(cm^{-1})	ratio
600-Nb_2O_5@NC−1	D Bond：1354.12 G Bond：1586.96	I_D/I_G =0.93
600-Nb_2O_5@NC-2	D Bond：1357.75 G Bond：1588.29	I_D/I_G =0.91
600-Nb_2O_5@NC-2.5	D Bond：1360.97 G Bond：1586.35	I_D/I_G =0.88
600-Nb_2O_5@NC-5	D Bond：1349.47 G Bond：1586.24	I_D/I_G =0.87
600-Nb_2O_5@NC−10	D Bond：1346.66 G Bond：1585.02	I_D/I_G =0.86
600-Nb_2O_5@C	D Bond：1351.55 G Bond：1592.81	I_D/I_G =0.86

Table S2. Brunauer-Emmett-Teller (BET) specific surface area and pore-size distribution of composite materials

Types of materials	Surface Area(m^2/g)	Average pore diameter(nm)
600-Nb_2O_5@C	182.69	4.14
600-Nb_2O_5@NC−10	190.67	4.53
600-Nb_2O_5@NC-5	180.95	4.31
600-Nb_2O_5@NC-2.5	130.27	4.17
600-Nb_2O_5@NC-2	136.67	4.98
600-Nb_2O_5@NC−1	60.75	5.32

Table S3. The chemical composition in atomic of nitrogen concentration derived from XPS peaks of 600-Nb_2O_5@NC-1, 600-Nb_2O_5@NC-2, 600-Nb_2O_5@NC-2.5, 600-Nb_2O_5@NC-5 and 600-Nb_2O_5@NC-10, respectively.

Types of materials	N(%)	Pyridinic N(%)	Pyrrolic N(%)	Graphitic N(%)
600-Nb_2O_5@NC−1	5.72	26.83	59.85	13.32
600-Nb_2O_5@NC-2	5.17	31.06	65.98	2.96
600-Nb_2O_5@NC-2.5	4.48	19.34	56.82	23.84
600-Nb_2O_5@NC-5	3.88	22.30	63.90	13.71
600-Nb_2O_5@NC−10	3.37	30.87	57.61	11.52

Table S4. Comparison of Nb_2O_5-based anodes in sodium-ion batteries

Electrode material name	Specific capacity at low rate	Specific capacity at high rate	Max cycle number	References
Nb_2O_5@3D PRS	271 mAh g^{-1} at 0.5 C	130 mAh g^{-1} at 10 C	7500	[1]
S-Nb_2O_5 HNS@S-rGO	215 mAh g^{-1} at 0.5 C	100 mAh g^{-1} at 20 C	3000	[2]
a-H-Nb_2O_5	185 mAh g^{-1} at 0.2 C	109 mAh g^{-1} at 5 C	3000	[3]
G-Nb_2O_5 nanosheets	230 mAh g^{-1} at 0.25 C	100 mAh g^{-1} at 20 C	1000	[4]
m-Nb_2O_5-C		175 mAh g^{-1} at 0.5 C	300	[5]
T-Nb_2O_5 / NCFs	196.8 mAh g^{-1} at 1 C	97 mAh g^{-1} at 40 C	5000	[6]
Nb_2O_5 NCs/rGO	242 mAh g^{-1} at 1 C	60 mAh g^{-1} at 50 C	5000	[7]
600-Nb_2O_5@ NC-2	280 mAhg^{-1} at 0.5 C	95.9 mAhg^{-1} at 50 C	3000	This work

Table S5. Fitting results of the data in Figure S10 with the simulated impedance parameters (*Rs*, *Rct*) obtained from the proposed equivalent circuit before and after 5th,50th,100th cycles of 600-Nb_2O_5, 600-Nb_2O_5@C and 600-Nb_2O_5@NC-2 anodes at a current density of 0.1 A g^{-1}

Sample	600-Nb_2O_5		600-Nb_2O_5@C		600-Nb_2O_5@NC-2	
	Rs (Ω)	Rct (Ω)	Rs (Ω)	Rct (Ω)	Rs (Ω)	Rct (Ω)
Before cycle	8.7	202.6	4	205.6	3.6	242.3
5th cycle	8.4	263.7	3.7	168.2	4.7	198.6
50th cycle	8.6	425.8	4.6	251.3	5.7	140.2
100th cycle	7.5	585.4	4.9	332.5	3.9	129.6

Reference

1. H. Yang, R. Xu, Y. Gong, Y. Yao, L. Gu and Y. Yu, *Nano Energy*, 2018, **48**, 448-455.
2. F. F. Liu, X. L. Cheng, R. Xu, Y. Wu, Y. Jiang and Y. Yu, *Adv. Funct. Mater.*, 2018, **28**, 1800394.
3. J. F. Ni, W. C. Wang, C. Wu, H. C. Liang, J. Maier, Y. Yu and L. Li, *Adv. Mater.*, 2017, **29,** 1605607.
4. L. Wang, X. F. Bi and S. B. Yang, *Adv. Mater.*, 2016, **28**, 7672-7679.
5. H. Kim, E. Lim, C. Jo, G. Yoon, J. Hwang, S. Jeong, J. Lee and K. Kang, *Nano Energy*, 2015, **16**, 62-70.
6. L. P. Yang, Y. E. Zhu, J. Sheng, F. Li, B. Tang, Y. Zhang and Z. Zhou, *small*, 2017, **13**, 1702588.
7. L. T. Yan, G. Chen, S. Sarker, S. Richins, H. Q. Wang, W. C. Xu, X. H. Rui and H. M. Luo, *ACS Appl. Mater. Interfaces*, 2016, **8**, 22213-22219.